Experimental Validation of Torque-Based Control for Realistic Handwheel Haptics in Driving Simulators

Damian, Mircea; Shyrokau, Barys; Carrera Akutain, Xabier; Happee, Riender

DOI
10.1109/TVT.2021.3125749

Publication date
2022

Document Version
Final published version

Published in
IEEE Transactions on Vehicular Technology

Experimental Validation of Torque-Based Control for Realistic Handwheel Haptics in Driving Simulators

Mircea Damian, Barys Shyrokau, Xabier Carrera Akutain, and Riender Happee

***Abstract*—A realistic steering feel is one of the key elements to guarantee fidelity on a driving simulator in general, and in particular to replicate on-centre vehicle handling. This requires precise modelling of the steering dynamics, a high bandwidth control loading system, and coupling of virtual and physical components in agreement with computational requirements and hardware limitations. For such a coupling, the common approach position-based control uses the measured signals of steering wheel angle and steering rate as inputs to the steering system model. This paper proposes an alternative torque-based control scheme using steering torque as an input to the steering system with additional compensation. Torque-based control was designed and evaluated in conjunction with detailed electric power steering models including state-of-the-art friction models, a neuromuscular driver model, and two driver-in-the-loop experiments in a high-end driving simulator. The objective analysis performed by means of the neuromuscular driver model reveals that the driver applies less impedance i.e. the driver is less stiff on a driving simulator when steering feedback is provided with the torque-based control compared to the position-based control. The investigations demonstrate that torque-based control reduces haptic response delay and vibrations caused by friction modelling compared to position-based control. The driver-in-the-loop experiments show significant objective effects on steering performance and subjective evaluation of fidelity and effort. We conclude that the proposed approach closes the vehicle-driver loop with more realism in a driving simulator.**

***Index Terms*—Steering feel, steering system, neuromuscular driver model, driving simulator, on-centre handling, subjective evaluation.**

I. Introduction

OVER the past decades, the technological improvements in computing power, software, and projection systems enabled driving simulators to become cost-effective tools to perform research activities. Nowadays driving simulators are widely used for studying the interaction of driver and vehicle systems, vehicle development, and human factors. They offer benefits naturalistic and instrumented vehicle studies with the main advantage being the versatility to configure virtual scenarios in a controlled and safe environment that matches the particular investigation requirements [1]: environmental conditions can be manipulated as state of the road surface, climate and day/ night operations; and the physical parameters of the driven vehicle can be altered e.g., steering characteristics, suspensions design and tire construction [2].

However, one of the key factors for the success of a driving simulator is its experimental validity [3], which is often explained in terms of physical and behavioral fidelity. Physical fidelity relates to the degree to which the simulator replicates the physical properties of the driving situation [4]. Behavioral fidelity instead refers to the simulators ability to evoke drivers behavior observed in the real world [5]. Physical and behavioral fidelity are strictly linked to each other and over the last years, simulator designers strived to reproduce high-quality visuals, auditory and kinesthetic cues in order to emulate the real driving experience. Complex motion platforms were developed to reproduce vehicles movements in the simulated environment, and numerous studies on the influence of motion proved that the use of motion cues improves the subjective quality of the simulator [6], [7]. Yet this comes at a higher cost and financial constraints may limit the simulators ability to fully stimulate the entire range of the drivers sensory modalities. Nonetheless, studies reported that if the simulators capabilities satisfy the research task and the user is absorbed in the simulated drive then the drivers control of the vehicle in the virtual environment is comparable to driving a real vehicle, and driving simulators could be employed to perform research activities [8].

A realistic steering feel is one of the key elements in order to replicate the on-center vehicle handling and achieve a good immersion on a driving simulator [9]. The hand-wheel feedback carries relevant correspondence regarding the instantaneous dynamics of the driven vehicle being physically related to the vehicles speed and trajectory and could be used by drivers to reinforce the visual information [10], [11]. Previous literature has extensively reported the importance of the steering feedback response in driving simulators [12]–[14]. However, little attention has been paid so far to create more realistic hand-wheel haptics. Moreover, the creation of a realistic steering feel is also an actual problem for steer-by-wire systems [15], where the upper control loop is similar to driving simulator steering system control.

The commonly used position-based control presents inherent stability issues caused mainly by the modelling of friction elements. These become very noticeable in the shape of steering

Manuscript received January 5, 2021; revised August 14, 2021; accepted October 13, 2021. Date of publication November 8, 2021; date of current version January 20, 2022. The review of this article was coordinated by Prof. Kanghyun Nam. *(Corresponding author: Barys Shyrokau.)*

Mircea Damian is with the Department of Cognitive Robotics, Delft University of Technology, Delft 2628CD, The Netherlands, and also with the Toyota Motor Europe, Zaventem 1930, Belgium (e-mail: Mircea.Damian@ro.bosch.com).

Barys Shyrokau and Riender Happee are with the Department of Cognitive Robotics, Delft University of Technology, Delft 2628CD, The Netherlands (e-mail: b.shyrokau@tudelft.nl; r.happee@tudelft.nl).

Xabier Carrera Akutain is with the Toyota Motor Europe, Zaventem 1930, Belgium (e-mail: Xabier.Carrera.Akutain@toyota-europe.com).

Digital Object Identifier 10.1109/TVT.2021.3125749

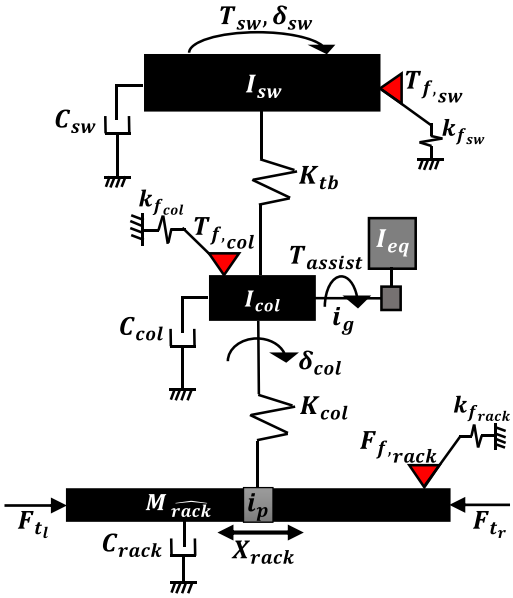

Fig. 1. Column EPS system model.

wheel vibrations, especially with low impedance. Consequently, drivers find it hard to execute precise maneuvers around the neutral position of the steering wheel. This paper extends the research done in [16] and exploits the potential of torque-based control to provide high-fidelity steering feedback in driving simulators, which will be essential to study Electric Power Steering (EPS) systems and will support general vehicle development.

The investigation results demonstrate that the proposed torque-based control reduces steering wheel oscillations and as confirmed by subjective evaluations enhances the on-centre handling steering fidelity in a driving simulator.

The structure of the article comprises the following sections. Section II presents the EPS system model used to simulate steering dynamics during the driver-in-loop experiments. Subsequently, Section III and IV describe the position-based and torque-based controls respectively. An objective evaluation of the two control strategies performed with a neuromuscular driver model is detailed in Section V, while the set-up of the driving simulator used during the driver-in-loop experiments is illustrated in Section VI. Thereupon Section VII, VIII, and IX present three distinctive driver-in-loop experiments carried out to compare the control strategies, and extensively describe the results. Finally, in the concluding part of the paper, the research findings are summarized and the outlooks for further development are denoted.

II. Steering System Model

In order to simulate and reproduce accurate characteristics of the steering wheel angle and steering wheel torque in driving simulators, a 3 Degree of Freedom (DoF) EPS system model was developed, characterizing a mid-size passenger car. It comprises all the mechanical components which transfer the steering wheel torque to the tie rods such as the steering wheel, torsion bar, steering column, assist electric motor, pinion, and rack. Fig. 1 shows its schematic layout including the steering wheel torque T_{sw}, the steering wheel angle δ_{sw}, the assist torque T_{assist} and the tie rod forces F_{tl}, F_{tr} which are provided by a non-linear vehicle model. In the figure I and M represent the rotational inertias and masses; K and C the stiffness and damping coefficients; T_f, F_f, and k_f correspond to friction torque/force and friction element stiffness; i_p the steering gear ratio; and i_g the motor gear ratio. The suffix sw indicates the steering wheel, tb the torsion bar, col the steering column, and $rack$ the rack guide.

Using Newton's second law of motion the steering wheel dynamics are derived as:

$$I_{sw}\ddot{\delta}_{sw} + C_{sw}\dot{\delta}_{sw} + T_{f,_{sw}} = T_{sw} - K_{tb}\big(\delta_{sw} - \delta_{col}\big) \quad (1)$$

Likewise the column dynamics for the case of column EPS type assist are formulated as:

$$\begin{aligned}&\big(I_{col} + I_{eq}i_g^2\big)\ddot{\delta}_{col} + C_{col}\dot{\delta}_{col} + T_{f,_{col}}\\ &= K_{tb}\big(\delta_{sw} - \delta_{col}\big) - K_{col}\Big(\delta_{sw} - \frac{X_{rack}}{i_p}\Big) + T_{assist}i_g \quad (2)\end{aligned}$$

K_{col} is the equivalent lower column, hardy disk and mesh stiffness. Finally, the rack dynamics are described as:

$$\begin{aligned}&M_{\widehat{rack}}\ddot{X}_{rack} + C_{rack}\dot{X}_{rack} + F_{f,_{rack}}\\ &= \frac{K_{col}}{i_p}\Big(\delta_{sw} - \frac{X_{rack}}{i_p}\Big) - F_{rack} \quad (3)\end{aligned}$$

In eq. (3) $M_{\widehat{rack}}$ is the sum of the rack mass and the suspensions inertia translated to the tie rods, while F_{rack} is the difference of left and right tie rod forces.

The remarkable influence of friction on steering behaviour and steering performance [17] imposes a need for accurate modelling of friction dynamics [18], where stick-slip leads to highly non-linear behaviour calling for small time-steps and dedicated friction models for efficient (real time) calculation. In order to model the effect of steering wheel and column friction the Exponential Spring Force Element (ESFE) friction model [11] is used, while to reproduce the rack friction dynamics with stick-slip behaviour three different friction sub-models are combined in parallel: ESFE models; linear model; and Reset Integrator model [19].

Friction velocity dependency is assumed to be of viscous type and modelled through viscous friction models. Steering mechanical parameters such as stiffness, damping, and friction were identified through quasi-static and dynamic steering bench tests and further validated with full vehicle testing. System's response with the EPS assist On/Off has a good correlation with experimental data with Pearson correlation coefficients above 0.98.

III. Position-Based Control

In driving simulators, the online coupling of virtual and physical steering components is enabled by the hand-wheel feedback command T_{req}^{CL} to the steering control loading system. The commonly used position-based control (PBC) strategy utilizes the measured steering wheel angle δ_{sw}^{CL} and steering wheel rate $\dot{\delta}_{sw}^{CL}$ to determine the control loading (CL) torque. Typical PBC generates the CL desired torque, based on the calculated upper

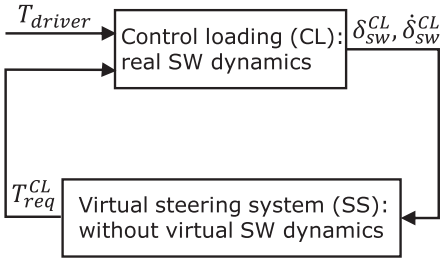

Fig. 2. Position-based control.

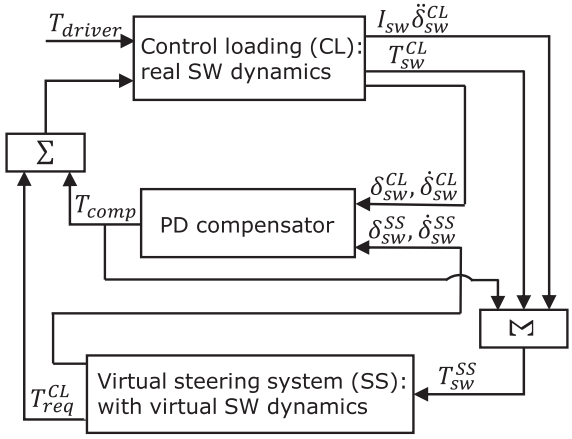

Fig. 3. Torque-based control.

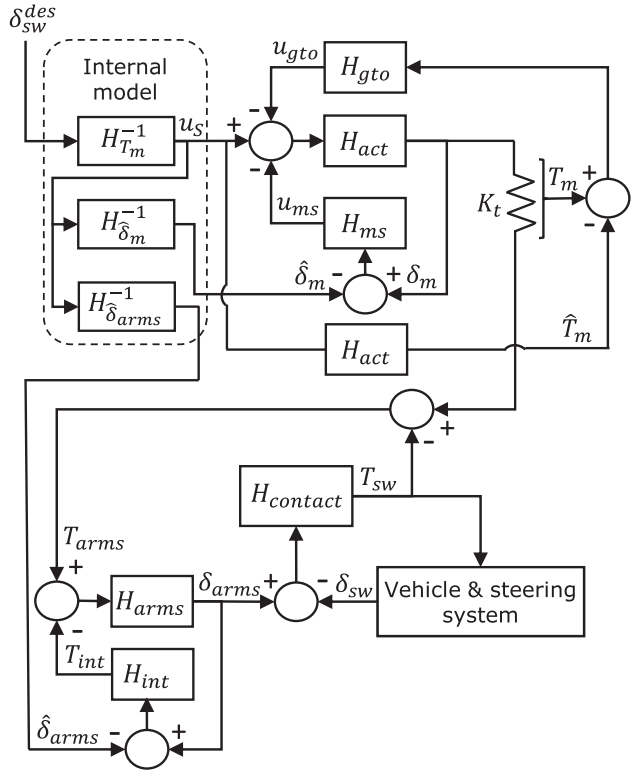

Fig. 4. Neuromuscular driver model.

column, steering wheel damping and steering wheel friction torques in the virtual steering system (SS) (Fig. 2):

$$T_{req}^{CL} = K_{tb}\left(\delta_{sw}^{CL} - \delta_{col}^{SS}\right) + C_{sw}\dot{\delta}_{sw}^{CL} + T_{f,_{sw}} \tag{4}$$

δ_{col}^{SS} is the virtual column angle, $T_{f,_{sw}}$ the steering wheel friction torque calculated based on measures from the control loading and C_{sw} the steering wheel damping.

The PBC control strategy when used real-time in driving simulators presents inherent stability issues caused mainly by computational latency and stiff model equations. These become noticeable in the form of torque feedback fluctuations and steering wheel vibrations which downgrade the quality and realism of the steering response.

IV. Torque-Based Control

The aforementioned stability issues have been solved through the implementation of a torque-based control (TBC) (Fig. 3). This strategy accounts for the virtual steering wheel dynamics and allows to simulate steering system model with different steering wheel inertia compared to the steering wheel mounted in the control loading.

The input to the virtual steering system is the torque applied by the driver, calculated as:

$$I_{sw}^{CL}\ddot{\delta}_{sw}^{CL} = T_{sw}^{SS} - T_{sw}^{CL} + T_{comp} \tag{5}$$

T_{sw}^{CL} is the torque measured from control loading, I_{sw}^{CL} the inertia of the steering wheel mounted in the control loading, $\ddot{\delta}_{sw}^{CL}$ the steering wheel acceleration and T_{comp} the compensated torque. Imposing torque balance at the level of the virtual steering wheel as in eq (1), a virtual steering wheel angle δ_{sw}^{SS} and virtual steering wheel rate $\dot{\delta}_{sw}^{SS}$ are computed and used in the model to calculate the steering wheel friction, steering wheel damping and upper column torques. The torque request to the control loading i.e. the steering feedback commanded to the electric motor is calculated based on the dynamics of the virtual steering system shown in Fig. 1 as follows:

$$\begin{aligned} T_{req}^{CL} &= K_{tb}\left(\delta_{sw}^{SS} - \delta_{col}^{SS}\right) + C_{sw}\dot{\delta}_{sw}^{SS} \\ &+ T_{f,_{sw}} + \left(I_{sw}^{CL} - I_{sw}^{SS}\right)\ddot{\delta}_{sw}^{SS} - T_{comp} \end{aligned} \tag{6}$$

In eq. (5) and (6) the compensated torque T_{comp} is required to minimize the mismatch between the dynamics of the virtual steering system model and the physical dynamics of the control loading, and is determined through a PD compensator:

$$T_{comp} = K_p\left(\delta_{sw}^{SS} - \delta_{sw}^{CL}\right) + K_d\left(\dot{\delta}_{sw}^{SS} - \dot{\delta}_{sw}^{CL}\right) \tag{7}$$

K_p is the proportional gain and K_d is the derivative gain.

V. Evaluation With a Neuromuscular Driver Model

Aiming to compare the previously described PBC and TBC control strategies, through offline simulations a risk-neutral [20] neuromuscular (NMS) driver model (Fig. 4) was developed, based on previous research performed by the Delft Laboratory for NeuroMuscular Control [21], [22] and the Vehicle Dynamics Group at Cambridge [23]–[25].

The NMS model includes neuromuscular feedback loops with delays, muscle activation dynamics, hand contact stiffness, and the inertia of the arms to predict realistic interactions including vibrations and oscillations. In this section, the NMS driver model structure is described for the case that no internal or

external disturbances affect the system's operation [22], [24]. Input sensor delay and control loading dynamics (external disturbances) are added to the driver-vehicle interaction to replicate the simulator's experimental conditions. Finally, comparative simulation results are presented and discussed.

A. NMS Driver Model Structure

The NMS model is illustrated in Fig. 4, and parameter values are in Table V in Appendix A. All signals and parameters are expressed in terms of steering wheel rotations and torques effectively lumping the left and right arms and the joints and muscles involved in steering. Parameters represent active control with both hands firmly holding the steer. We assume that the driver controls the vehicle path dictating the steering angle, using neuromuscular position feedback originating from the muscle spindles. The input to the NMS driver model is the angle δ_{sw}^{des} that the driver desires to apply at the steering wheel interface. This is assumed to be provided by higher neural paths. Given δ_{sw}^{des}, the central nervous system determines the feedforward muscle torque required to reach the desired angle through inverse internal dynamics model H_{Tm}^{-1}, that signifies driver's mental representation of the vehicle, steering and NMS dynamics [26]. Using this feedforward control the NMS model will exactly realize δ_{sw}^{des} if there are no internal or/and external disturbances affecting system's operation and the commanded motion does not exceed the NMS bandwidth [22], [27]. In addition, the CNS adjusts the arms impedance through co-contraction and sensory feedback in order to reach δ_{sw}^{des} using so called impedance control [21], [26]. In Fig. 4, the output of H_{Tm}^{-1} is a supraspinal signal representative of the feedforward muscle torque to be applied. This is combined with muscle stretch and stretch velocity feedback from muscle spindles H_{ms}, and force feedback from the Golgi tendon organ H_{gto}. Both reflexive pathways are characterized by a spinal delay time τ_{spin} which limits their effective bandwidth:

$$H_{ms} = (K_{spin} + C_{spin}s)e^{-s\tau_{spin}} \tag{8}$$

$$H_{gto} = K_{gto}e^{-s\tau_{spin}} \tag{9}$$

The muscle spindle feedback is a function of the error between actual and desired joint angles and velocities i.e. $\delta_m, \dot{\delta}_m$ and $\hat{\delta}_m, \dot{\hat{\delta}}_m$ respectively. The latter is estimated by the human central nervous system through the inverse internal dynamics model. The Golgi tendon organ feedback, function of the actual muscle torque T_m and the desired muscle torque $\hat{T}_m$, is assumed zero in the current study but will be relevant in tasks where humans control force or admittance [27], [28].

Consequently, the collective signal from the internal model and reflexive pathways travels through the nervous system to the muscles, where it is converted into torque by the contractile element. In order to account for the motor neurons finite transmission velocities and muscle fiber activation delay, the input is filtered with a second-order low pass filter [29]–[31]:

$$H_{act} = \frac{\omega_o^2}{s^2 + 2\zeta\omega s + \omega_o^2} \tag{10}$$

Instantaneous visco-elastic proprieties from already co-contracted arms are contained in,

$$H_{int} = K_{int} + C_{int}s \tag{11}$$

whereby the driver can increase the limbs stiffness and damping in order to reduce the error between actual and expected arms angles and velocities [21], [26] i.e. $\delta_{arms}, \dot{\delta}_{arms}$ and $\hat{\delta}_{arms}, \dot{\hat{\delta}}_{arms}$ respectively.

The net torque input accelerates the arms inertia

$$H_{arms} = \frac{1}{I_{arms}s^2} \tag{12}$$

resulting in the arms angle δ_{arms}. This is equivalent to the steering wheel angle δ_{sw} if the driver applies an infinitely stiff grip. However, this is not the case since the driver's hands have finite visco-elastic proprieties which have been accounted in:

$$H_{contact} = K_{hands} + C_{hands}s \tag{13}$$

The output of the contact dynamics is the torque T_{sw} that the driver applies at the steering wheel interface.

The internal model transfer functions are derived for the case of a single track vehicle model coupled with a linear column EPS system (Fig. 4) and no disturbances affect system's operation as [27]:

$$H_{T_m}^{-1} = \frac{u_S}{\delta_{sw}^{des}} \text{ with } (H_{ms} = 0, H_{int} = 0, H_{gto} = 0) \tag{14}$$

$$H_{\hat{\delta}_m} = \frac{\hat{\delta}_m}{u_S} \text{ with } (H_{ms} = 0, H_{int} = 0, H_{gto} = 0) \tag{15}$$

$$H_{\hat{\delta}_{arms}} = \frac{\hat{\delta}_{arms}}{u_S} \text{ with } (H_{ms} = 0, H_{int} = 0, H_{gto} = 0) \tag{16}$$

The values of the NMS system parameters used for simulations are shown in Appendix A.

B. Simulation Conditions

In order to emulate the simulator's experimental conditions, input delays, and control loading dynamics (external disturbances) are added to the driver-vehicle interaction as depicted in Fig. 5.

d_a represents the sensor angle delay (10 ms), d_t the sensor torque delay (15 ms), and H_{CL} steering actuator's dynamics which are modelled through a first order filter of cut-off frequency ω_{CL} (30 rd/s) as:

$$H_{CL} = \frac{\omega_{CL}}{s + \omega_{CL}} \tag{17}$$

C. Results

To investigate the differences in system's response when steering feedback is provided with the PBC and with the TBC, two simulation scenarios are tested being sine steering (Fig. 6) and a lane change (Fig. 7). Both scenarios adopt a vehicle speed of 100 km/h and a time step of 1 ms aiming to emulate the real time experience.

Fig. 6 presents the simulation results for the case the input to the NMS driver model i.e. δ_{sw}^{des} is a sine steering wheel

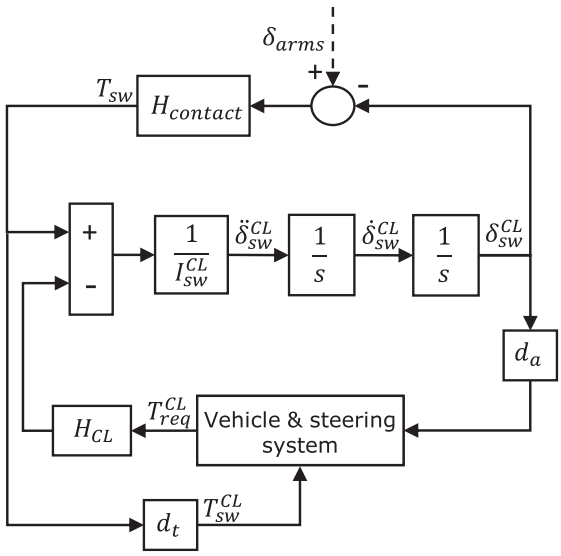

Fig. 5. Simulator experimental conditions.

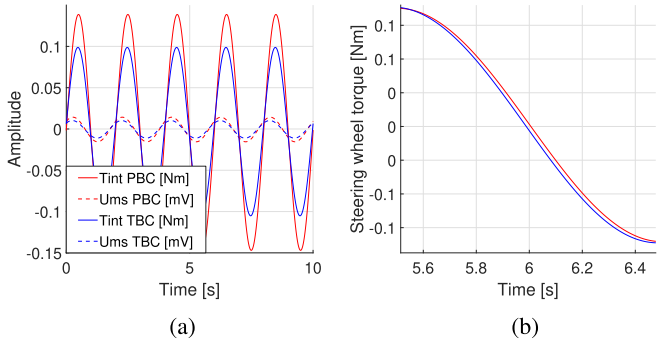

Fig. 6. Sine maneuver (red line PBC, blue line TBC). (a) NMS model feedback. (b) Steering wheel torque.

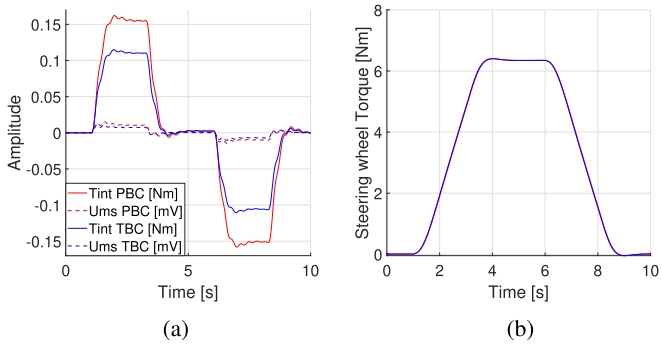

Fig. 7. Lane change maneuver (red line PBC, blue line TBC). (a) NMS model feedback. (b) Steering wheel angle.

angle of amplitude 8 deg and frequency 0.5 Hz. The left figure (Fig. 6(a)) depicts the NMS feedback from muscle spindles (dashed line) and co-contraction (continuous line) and the right figure (Fig. 6(b)) the applied steering wheel torque T_{sw} in the interval of time 5.5 - 6.5 s. In the former, it is observed that the driver increases impedance through co-contraction and feedback in order to compensate for the external disturbances, i.e. sensor delay and control loading dynamics, and reach the desired steering wheel angle. Additionally, it is noted that the NMS feedback amplitude is smaller with the TBC compared to the PBC. The compensation scheme of the TBC compensates for the external disturbances, in particular the control loading dynamics, resulting in smaller NMS feedback applied by the driver and smaller haptic delays (Fig. 6(b)).

Fig. 7 illustrates a lane change maneuver simulation in which the driver applies a steering wheel angle of amplitude 60 deg at about 20 deg/s. In line with the above results the NMS feedback amplitude, therefore the impedance of the driver, is smaller with the TBC compared to the PBC (Fig. 7(a)), although the driver applies the same steering angle and steering wheel torque profile with both control strategies (Fig. 7(b)).

The presented simulations' outcome is not perceptible for the case in which the time step is reduced by a factor of 10, and vanishes, when motor dynamics and sensor delays are not included in the developed model, i.e. the TBC and PBC are equivalent when an ideal system is used, and both converge to the correct solution. The objective analysis performed by means of the NMS driver model reveals that the driver is less stiff on a driving simulator when steering feedback is provided with the TBC compared to the PBC. The compensation scheme compensates for the control dynamics and haptic delays resulting in a more natural steering feel.

VI. Driving Simulator

In order to assess controllers' performances in a driving simulator, two sets of driver-in-loop (DIL) experiments were performed. These were conducted in the driving simulator located at Toyota Motor Europe. It consists of a static mock-up with a 210-degree projection screen. The instrument dashboard communicates vehicle information to the driver, such as speed and engine rpm, while a sound system provides audio to create a more immersive experience. The force feedback is generated by an AC brushless electric motor and connected to the steering wheel at the approximate position of the virtual torsion bar. The maximum continuous and peak torque of the actuator are respectively 21 Nm and 30 Nm. Additionally, the steering actuator provides a high-resolution displacement measurement with an accuracy of $<0.1\,^{\circ}$ and torque measurement with an accuracy of <0.1 Nm. A multi-node PC configuration is established through UDP-TCP communication in soft real-time (RT) and hard RT at 1 kHz. rFPro toolchain is used to generate the environment physics and create a visual scenario through scene rendering at a frequency of 100 Hz. The vehicle dynamics are modelled in IPG CarMaker and steering system's dynamics in Simulink, both running at 1 kHz. The system is equipped with a dSPACE DS1006 which enables to perform experiments in hard real time as an alternative to soft real-time, where the completion of the periodic deadlines cannot be guaranteed.

VII. Haptic Feedback and Stability Study With ISW

The first set of DIL experiments were performed with an instrumented steering wheel (ISW) [32] (Fig. 8). This device is able to measure the forces and grips that the driver applies

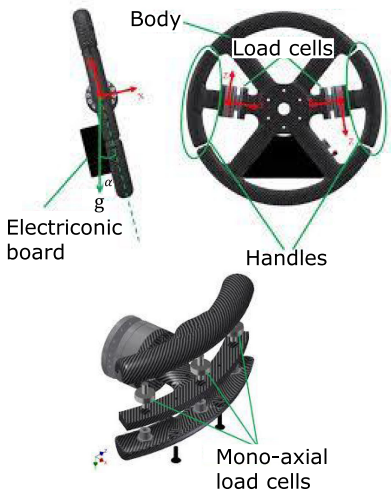

Fig. 8. Instrumented steering wheel.

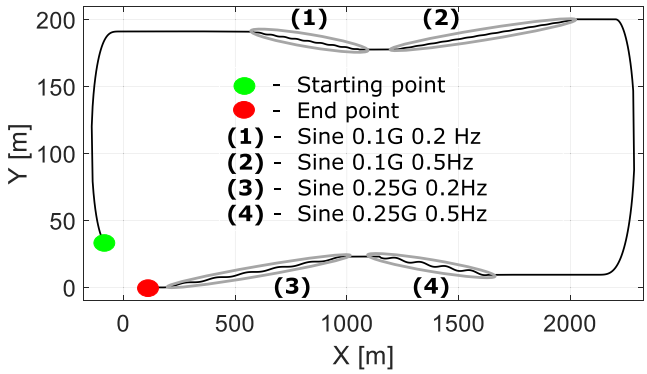

Fig. 9. Track for the first set of DIL experiments.

at the steering wheel interface with high accuracy. The objective was to investigate the differences in the forces and grips applied by the driver at the hand-wheel when steering feedback is calculated using the PBC and the TBC. In this section, the experimental design is described, followed by the main findings and a discussion.

A. Participants

Four expert evaluators belonging to different chassis development departments at Toyota Motor Europe took part in this experiment. Participants had an average age of 38 years, a standard deviation (SD) of 8 years, and had a driving license for 15 years (SD=3.36).

B. Driving Route

The experimental track was a wide flat road environment with steady weather conditions (Fig. 9). The driving route was marked with red cones and was 4.5 Km long. It consisted of 4 sine sections, 5 straight line sections and 2 high radius corners. The sine sections were characterized by the amplitudes of the steering wheel corresponding to levels of lateral acceleration about 1 m/s^2 - 2.5 m/s^2 and frequencies of 0.2 Hz - 0.5 Hz. The route was designed aiming to test the two controllers both in centre-handling on the straight sections and in more dynamic steering on the sine and high-radius corner sections.

C. Experimental Design

Experiments were performed in hard RT with two EPS assist logics, hereafter named EPS 1 and EPS 2, while steering feedback was calculated using the PBC and the TBC based on the dynamics of the virtual steering system model. The overall experiment lasted 4 days i.e. one for each driver. During the experiment, a nominal speed of 100 km/h was supported by cruise control as the objective was to examine drivers' steering control. The driving task was to follow as close as possible the driving route marked with red cones. Participants were invited to take part in the experiment separately in order to avoid bias of results and to drive four laps of the route i.e. two with EPS 1 and two with EPS 2 in random order. The drivers had no knowledge regarding the configuration that was tested. After driving the first two configurations, where the difference between the former and the latter was the control strategy used to calculate the hand-wheel feedback i.e. PBC or TBC, drivers were asked to report their subjective impressions and compare the two configurations. The aim was to obtain meaningful indications regarding controllers' performances and allow the driver to take a short break which on average has been about 5 to 10 minutes. Following, they were invited to do the same for the last two configurations (for an extensive application with the ISW refer to [33]).

D. Results

Analysis was performed both on raw and averaged forces and grips signals per sine section (Fig. 10). However, no common trend could be identified. There was a substantial inter and intra subject variability in the measured signals.

Nonetheless, during the experiment participants declared to perceive significant vibrations at the steering wheel interface with the position-based control. Conversely, these were absent with the torque-based control. In order to investigate this phenomenon, the forces measured by the ISW were used to calculate the steering wheel torque, and the power spectral density (PSD) of this signal was computed. Fig. 11 shows the aforementioned PSD for the case of low driver impedance. The reduction in steering wheel vibrations with the TBC is evidenced by decreased power above 5 Hz in the calculated torque signal.

E. Discussion

Upon analysis of the data collected with the ISW experiment on average no differences were identified in driver forces and grips when steering feedback was computed using the PBC or the TBC. This is suspected to be due to the limited amount of experimental data and drivers' experience i.e. the expert evaluators have knowledge of the simulator's controls and on average achieve similar driving performances with the two algorithms. However, drivers declared to perceive a significant amount of steering wheel vibrations when feedback was calculated using the PBC. Contrarily, these were absent with the TBC. The

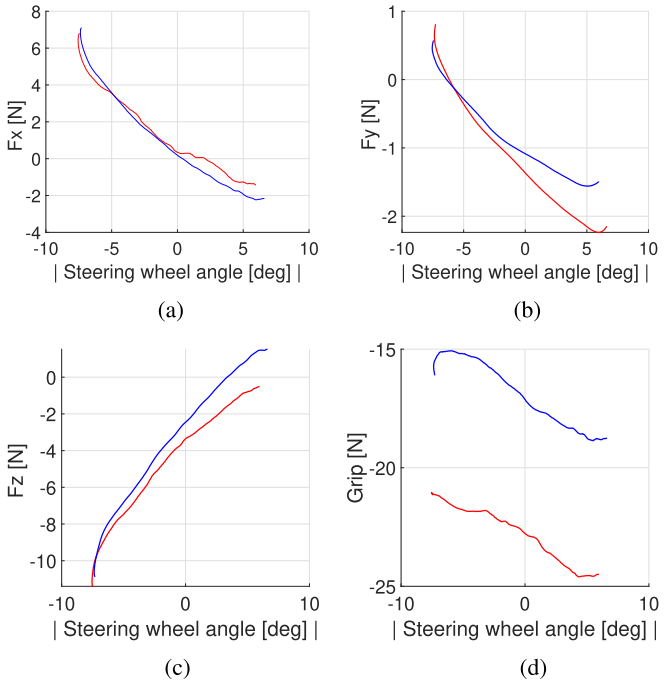

Fig. 10. Average ISW signals - left hand (red line PBC, blue line TBC). (a) Applied longitudinal force F_x. (b) Applied lateral force F_y. (c) Applied vertical force F_z. (d) Grip force

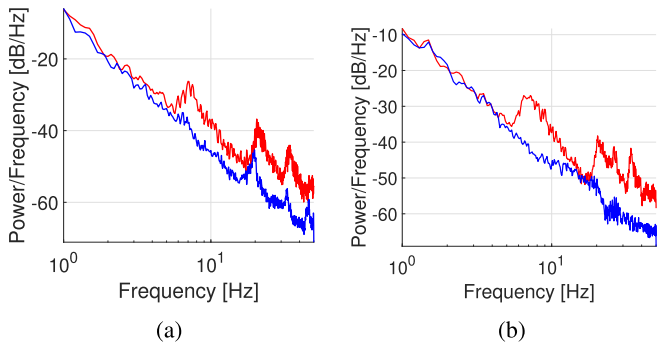

Fig. 11. PSD steering wheel torque ISW (red line PBC, blue line TBC). (a) EPS 1. (b) EPS 2.

subjective evaluations were confirmed by computing the power spectral density of the torque signal measured at the steering wheel interface. After completion of the experiment, following a detailed analysis of the simulated SS dynamics, it was found that the steering wheel vibrations experienced by the drivers when steering feedback is provided with the PBC are caused by drops in the simulated steering friction signals (Fig. 12). As already proved by previous research, friction has a critical influence on system's response fidelity and stability [18], [34]. Advanced friction models are required to assure good matching with experimental data but stiff model equations and a too high computational effort degraded the rendering of steering feedback, resulting in steering wheel vibrations and torque feedback fluctuations. Such phenomenon is highly noticeable in the case of low driver impedance, especially, during on-centre maneuvers with small target corrections of steering wheel angle.

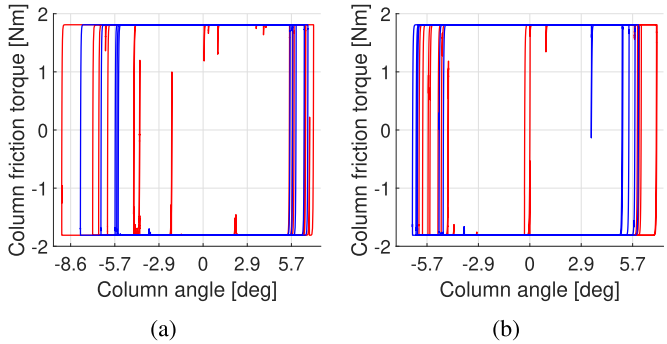

Fig. 12. Column friction (red line PBC, blue line TBC). (a) EPS 1. (b) EPS 2.

The expert evaluators, during the experiment, argued additionally that the complete suppression of steering wheel vibrations and oscillations, and the absence of "road vibration noise" could generate a "flat" artificial steering feel for the TBC. Therefore, in order to create more realistic hand-wheel haptics, an artificial noise was added. In this strategy, TBC + noise, disturbances are added to the control loading request, based on internal investigations performed at Toyota Motor Europe, aiming to improve steering feel and provide drivers with the claimed road feel.

VIII. Stability Study With Accelerometers

The power spectral density of the torque signal as computed in Fig. 11 could be dependent not only on the system's performance but even on the level of grip with which the driver holds the steering wheel. Therefore, to objectively compare the stability performance of the described algorithms and measure the intensity of the transmitted vibrations, three analogue uniaxial accelerometers of type Kiowa 2 G were mounted on the simulator steering shaft and experiments were performed both in soft RT and in hard RT. Accelerometer measurements were acquired through an Ipetronik device at 100 Hz operating with the IPEmotion RT software, while driving on the route shown in Fig. 9, and transmitted to the data logger PC by Vector CAN.

Analysis of the collected data in the experiment revealed that the stability issues induce resonance peaks in the torque measured from control loading which translates into torsional vibrations (Fig. 13). Moreover, the amplitude of the resonance peaks and signals' power is greater in soft RT experiments compared to hard RT experiments, and when the EPS 1 logic is used to supply assistance torque in the virtual model. The TBC ensures higher hand-wheel stability compared to the PBC but the difference is more noticeable in hard RT experiments, where the resonance peaks are almost absent with TBC. However, as reported by the expert evaluators the absence of steering wheel vibrations could lead to an artificial steering feel for TBC in hard RT. The countermeasure has been to implement the TBC+noise. In Fig. 13 it is observed that this strategy attenuates the resonance peaks alike the torque-based control but additionally provides the road feel claimed by the drivers in the ISW experiment.

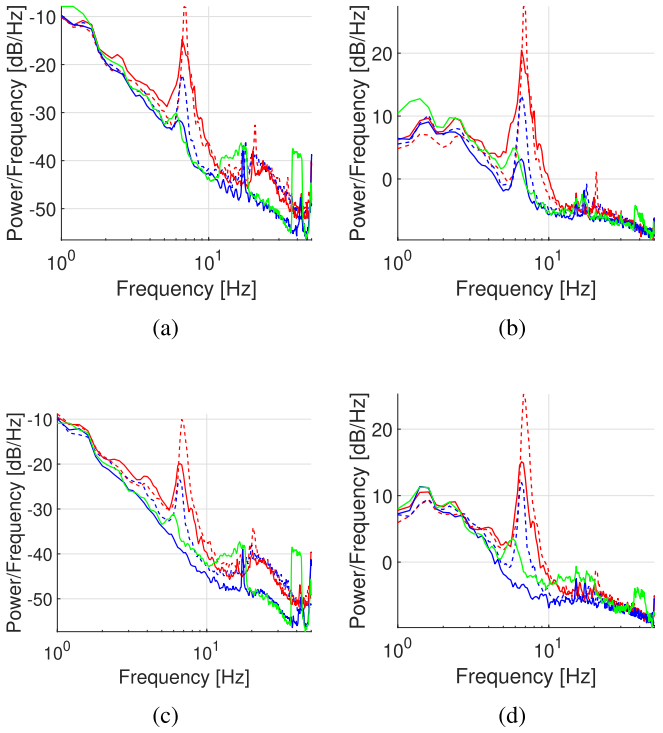

Fig. 13. Stability study - Power spectral density (red dashed line PBC soft RT, blue dashed line TBC soft RT, red continuous line: PBC hard RT, blue continuous line - TBC hard RT, green continuous line TBC+noise hard RT). (a) Torque measured from CL, EPS 1. (b) Torsional vibration (accelerometers), EPS 1. (c) Torque measured from CL, EPS 2. (d) Torsional vibration (accelerometers), EPS 2.

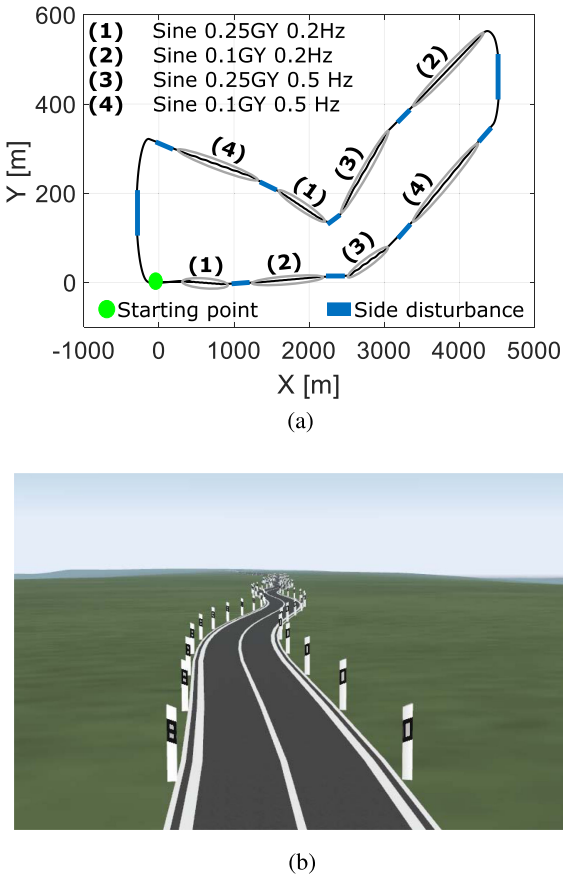

Fig. 14. DIL driving route. (a) Track for the second set of DIL experiments. (b) Road sine section.

IX. Steering Feedback Subjective Assessment

The objective of the second set of DIL experiments was to assess algorithms' performances from drivers' perspective and further investigate the effect of the system's instabilities on drivers' steering control. The following section presents the experimental design and results obtained.

A. Participants

The test group consisted of 8 drivers with an average age of 32 years (SD=7.36). Drivers were recruited from different departments responsible for steering development and assessment at Toyota Motor Europe. Among them, two were expert evaluators. On average participants had a driving license for 13 years (SD=7.56). Professional drivers provide more consistent evaluation compared to less experienced ones [35], therefore, the test group was limited to experienced drivers involved in the EPS development and evaluation.

B. Driving Route

The 4.5 km long driving route used in the ISW study was too short to allow non-professional drivers to reliably assess controllers' performance. Therefore, a new 10 km long driving route was designed for the second DIL experiment. It consisted of 8 sine sections, 6 straight line sections, and 2 high radius corners, as depicted in Fig. 14(a). The sine sections were characterized by the amplitudes of the steering wheel corresponding to levels of lateral acceleration about 1 m/s^2 - 2.5 m/s^2 and frequencies of 0.2 Hz - 0.5 Hz, similar to the previous experiment.

In the ISW experiment the driving route was marked with red cones. However, it was observed that these were difficult to follow visually and some drivers imprecisely followed the low frequency sine sections. Therefore, the driving track was completely redesigned. A new road was created which follows the shape of the desired driving route which was marked with a white line on the middle of the road, as shown in Fig. 14(b). The road width was 10 m on the straight line sections and only 3 m on the sine sections to constrain the driver to follow the path. An additional vehicle motion disturbance was generated as step-wise side wind gusts with a wind speed of 70 km/h along the straight line and corner sections. The aim was to determine with which of the three algorithms drivers' steering control is more stable and participants can better command vehicle's dynamics in order to follow the drivers' route.

C. Experimental Design

Experiments were performed in hard RT with the PBC, the TBC and the TBC with added noise. The experiment driving task was to follow as close as possible the driving route at a nominal speed of 100 km/h with cruise control. The test procedure included pre-driving instructions and a training session to

accustom the driver to the driving simulator. Specifically, prior to the start of the experiment drivers were informed that they must compare three steering feedback control strategies and the experimental design was explained. Additionally, the driving route and the subjective questionnaire that participants had to fill were presented.

In the training session evaluators drove only one lap of the route without step-wise side wind gusts disturbance and steering feedback was provided using the PBC.

Subsequently to the training session, participants drove two consecutive laps of the route, one for each control, i.e. PBC and TBC, on single blind mode at random order to avoid bias of results. The type of control was changed online after the end of the first lap and drivers were explicitly informed of the switch but without knowledge of the corresponding control method selection. At the end of the session drivers had a 5-min break and were asked to complete two evaluation forms, i.e. one for each type of control, referred as 1 and 2. Following the completion of the evaluation form, participants drove again two laps of the route. During one lap steering feedback was provided using the PBC, while in the other lap TBC with added noise (TBC+noise) was used, in a randomized order. Evaluators were informed that they would drive one lap with one of the previous control approaches and one lap with the new control defined as 3. This allows the driver to have always a valid reference, i.e. the PBC, for a more consistent assessment. The participants were asked to fill the same evaluation form for the second subset.

D. Objective Indicators

In order to evaluate drivers' performance and effort when feedback is provided with the three control methods, the following objective indicators are used:

MSE: mean steering effort (Nm · deg) as an indicator of steering effort [36];

SDLC: standard deviation of lateral position (m) from road centre line as performance indicator [37];

SE: steering entropy [38] to assess driver workload based on SAE J2944 [39];

SRR: steering wheel reversal rate (per minute) to assess driver workload based on SAE J2944;

rmsST: root-mean-square of steering torque (Nm) as an indicator of steering effort;

Angle (deg) and Torque hysteresis (Nm): as indicators of steering friction [40].

E. Subjective Indicators

In addition to the objective indicators, a questionnaire was developed based on the results found during the pilot study, steering feel evaluation procedures [41] and internal TME recommendations aiming to support the objective indicators and investigate drivers' feel. The total number of questions was 5 and all were formulated in English. The following questions were presented on an evaluation sheet on a 7-point scale with anchors:

Overall effort: how hard did you have to work to accomplish your level of performance during the line following task? The anchors are at 1-2 (very low), 3-5 (neither), 6-7 (very high).

The aim is to asses if systems instabilities i.e. torque fluctuations and steering wheel oscillations affect drivers' perceived effort when accomplishing the line following task.

Solidity on centre: how solid was your steering behaviour around on centre? The anchors are at 1-2 (slack), 3-5 (neutral), 6-7 (stuck).

This question is formulated to better understand drivers' attitude in steering control when feedback is provided with the three control methods. In particular, if the driver has to provide extra damping with his own limbs in the sine sections.

Holding precision in large corners: how precise was the steering wheel holding when driving through the large corners? The anchors are at 1-2 (inaccurate), 3-5 (normal), 6-7 (very precise).

Controllers' performances deteriorate in quasi-static manoeuvres. The objective is to determine which of the three strategies performs better in these conditions.

Vibrations/Oscillations: how much vibration steering wheel oscillations you perceived? The anchors are at 1-2 (no vibrations), 3-5 (normal), 6-7 (too much vibration).

This question aims to quantify the amount of perceived steering wheel vibrations/oscillations i.e. investigate this phenomenon from drivers' perspective.

Overall steering realism: how realistic was the steering setting? The anchors are at 1-2 (was like a joystick), 3-5 (neither), 6-7 (was realistic).

The objective is to establish which control strategy provides a more natural feel that resembles the actual vehicle's steering performance.

F. Results

Statistical significance of the results was assessed using an analysis of variance (ANOVA), comparing the three feedback control methods. A parametric test (ANOVA) was used because all data was expected to be normally distributed across participants. Homoscedasticity was further checked using Bartletts test. Results were declared statistically significant when the p-value is lower than 0.05. However, as a robustness check, all ANOVAs were repeated using the rank-based nonparametric Kruskal-Wallis test (Appendix B). Moreover, outliers were discarded according to Chauvenets criterion [42]. The mean values and standard deviation of subjective and objective indicators, and their statistically significance are reported in Tables I - IV. Subjective indicators and statistically significant objective indicators are also plotted using box plots in in Fig. 15 (Appendix C).

G. Discussion

The second DIL study investigated the potential of the proposed TBC to provide steering feedback in a driving simulator. Its performance was compared to the commonly used PBC.

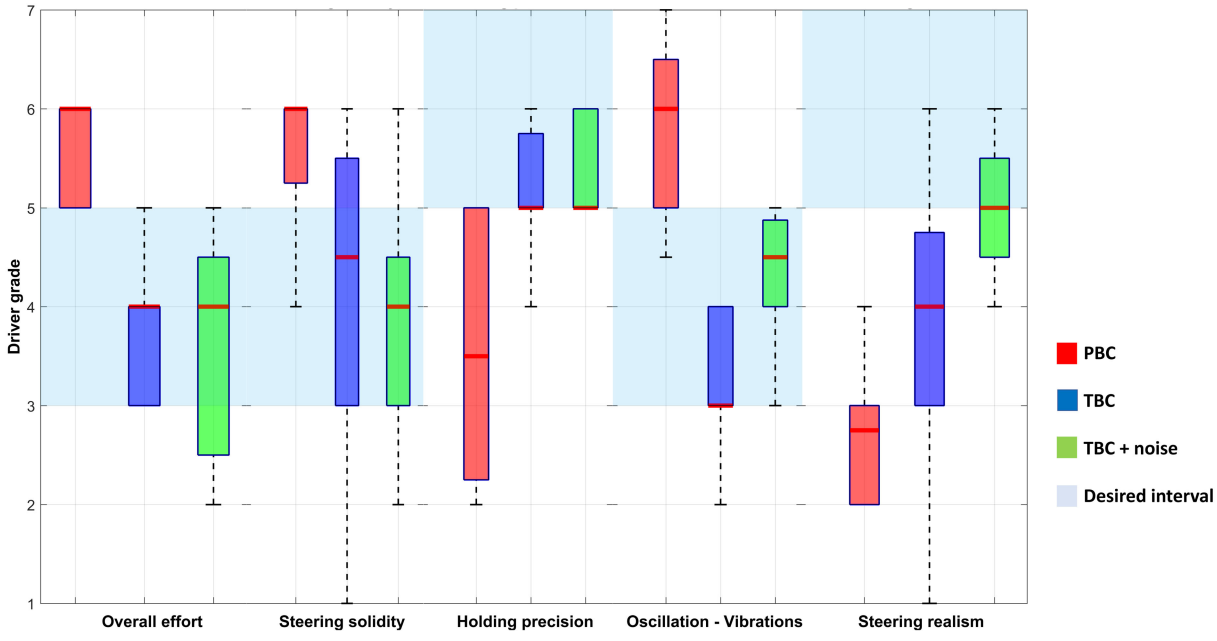

(a)

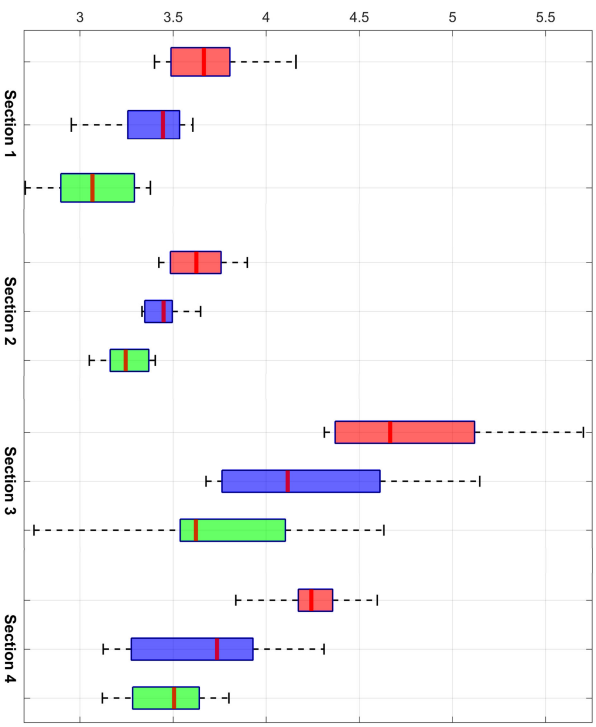

(b)

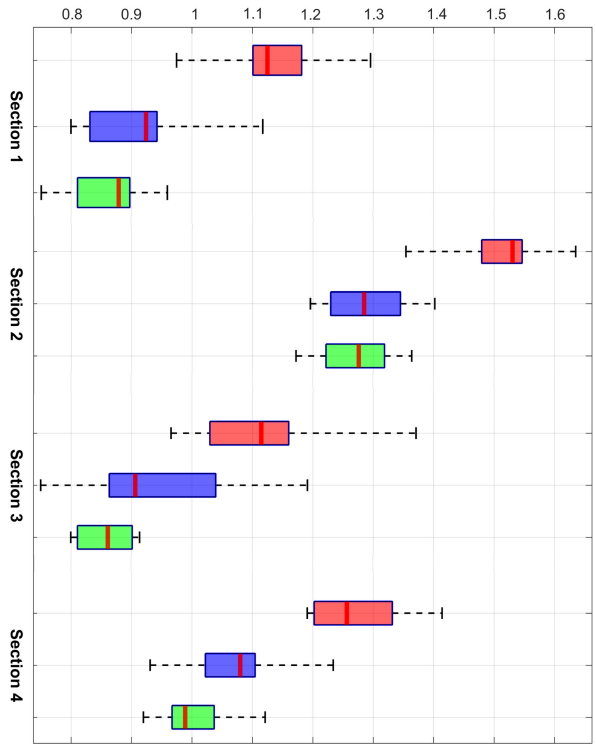

(c)

Fig. 15. Box plots subjective & objective data.

TABLE I
OBJECTIVE DATA OVERALL TRACK

Par	PBC	TBC	TBC + noise	F	p
MSE	22.09 (2.18)	22.02 (2.03)	22.45 (2.02)	0.10	0.90
SDLC	0.66 (0.06)	0.62 (0.06)	0.65 (0.07)	0.66	0.53
SE	0.72 (0.06)	0.73 (0.07)	0.74 (0.06)	0.17	0.85
SRR	26.2 (5.2)	24.5 (4.4)	25.7 (4.5)	0.24	0.78
rmsST	1.92 (0.10)	1.91 (0.09)	1.93 (0.08)	0.06	0.94

TABLE II
ANGLE HYSTERESIS SINE SECTION

Section	PBC	TBC	TBC + noise	F	p
1	3.69 (0.25)	3.38 (0.23)	3.07 (0.25)	**11.8**	**0.001**
2	3.63 (0.17)	3.44 (0.11)	3.25 (0.12)	**13.6**	**0.001**
3	4.8 (0.51)	4.22 (0.54)	(3.74) (0.55)	**7.3**	**0.004**
4	4.24 (0.25)	3.66 (0.41)	3.47 (0.24)	**10.8**	**0.001**

TABLE III
TORQUE HYSTERESIS SINE SECTION

Section	PBC	TBC	TBC + noise	F	p
1	1.13 (0.09)	0.91 (0.1)	0.86 (0.07)	**20.6**	**0.001**
2	1.51 (0.08)	1.29 (0.07)	1.27 (0.06)	**23.4**	**0.001**
3	1.12 (0.13)	0.94 (0.14)	0.86 (0.05)	**10.5**	**0.001**
4	1.27 (0.08)	1.07 (0.09)	1.01 (0.06)	**19.4**	**0.001**

On average participants shared acceptance toward the TBC with added noise as a method for providing steering feedback in driving simulators and judged the steering realism with this method up to 46% more realistic than with the traditional PBC. They reported a higher level of perceived steering wheel vibrations with the TBC with added noise compared to the TBC due to the synthetic addition of noise. However, this generally was preferred. All participants reported a spring-like feel when steering feedback was provided using the PBC and imprecision in holding the steering wheel in large corners. They claimed to feel a resistance force pulling the steering wheel toward the centre position. Additionally, they declared difficulty in centring the steering wheel around a neutral centre and perceived a significant amount of vibrations at the steering wheel for the PBC. They judged their steering behaviour up to 30% more stuck with the PBC compared to the proposed one. Objectively this is reflected in an increase of angle and torque hysteresis up to 1 deg and 0.27 Nm when steering feedback is provided with the PBC. Moreover, the participants reported a decrease in the overall effort up to 35.7% with the proposed TBC compared to the traditional PBC. Statistical insignificance of objective performance for overall error and effort indicators can be explained by the participants being able to adapt their steering behaviour and handle the task at the expense of a higher perceived workload. This realistic application study showed no difference in performance between the three steering control loading methods. However, profound differences were observed in the angle hysteresis, torque hysteresis and subjective evaluation. This proves the importance of steering control loading in studies evaluating handling qualities.

TABLE IV
SUBJECTIVE DATA

Criteria	PBC	TBC	TBC + noise	F	p
Overall effort	5.6 (0.52)	3.7 (0.76)	3.6 (1.19)	**13.2**	**0.001**
Steering solidity	5.6 (0.79)	4.1 (1.73)	3.9 (1.25)	3.5	0.05
Holding precision	3.6 (1.38)	5.1 (0.69)	5.4 (0.53)	**7.3**	**0.005**
Vibrations	5.8 (0.92)	3.3 (0.76)	4.3 (0.70)	**18.9**	**0.001**
Steering realism	2.7 (0.70)	3.8 (1.51)	5.0 (0.76)	**9.6**	**0.01**

As motivated in the above simulations with the neuromuscular control model we deem the TBC to better represent the actual vehicle dynamic response and the subsequent haptic feedback. Adding noise was proven to further enhance realism, where instead of the current predefined noise, it could be explored to simulate physical sources including tyre road interaction.

X. OVERALL CONCLUSION

In conclusion, this investigation has proven that friction models used in the virtual system strongly affect steering fidelity and stability in driving simulators. As already reported by previous literature advanced friction models are required to assure good matching with experimental data. However, stiff model equations and computational and hardware limitations lead to drops in the simulated friction signals, which translate into torque feedback fluctuations and steering wheel oscillations. Consequently, these affect drivers' feel and could evoke unrealistic behaviour. As confirmed by subjective evaluations, the proposed torque-based control strategies reduce steering wheel oscillation and enhance the steering fidelity in a driving simulator. In particular,

TABLE V
NMS SYSTEM PARAMETERS

Par.	Value	Source
ω_o	2.17 · 2 ·π [rad/s2]	[22], [27], [29], [31]
ζ	0.74 [-]	[22], [27], [29], [31]
K_t	30 [Nm/rad]	[24]
K_{spin}	4 [Nm/rad]	[22], [27]
C_{spin}	1.65 [Nm/rad/s]	[22], [27]
τ_{spin}	20 [ms]	[22], [27]
K_{gto}	0 [Nm/rad]	[22], [27]
I_{arms}	0.16 [kg m2]	[22], [27]
K_{int}	52.5 [Nm/rad]	[22], [27]
C_{int}	0.85 [Nm/rad/s]	[22], [27]
K_{hands}	600 [Nm/rad]	[22], [27]
C_{hands}	13 [Nm/rad/s]	[22], [27]

TABLE VI
KRUSKAL-WALLIS TEST - OBJECTIVE DATA OVERALL TRACK

Par	**PBC**	**TBC**	**TBC + noise**	**H**	**p**
MSE	22.09 (2.18)	22.02 (2.03)	22.45 (2.02)	0.10	0.95
SDLC	0.66 (0.06)	0.62 (0.06)	0.65 (0.07)	1.06	0.59
SE	0.72 (0.06)	0.73 (0.07)	0.74 (0.06)	0.34	0.89
SRR	26.2 (5.2)	24.5 (4.4)	25.7 (4.5)	0.78	0.68
rmsST	1.92 (0.10)	1.91 (0.09)	1.93 (0.08)	0.11	0.94

the control approach results in a clear improvement of steering feedback rendering around pure on-centre compared to position-based control. We uniquely complemented torque-based control with a compensator loop to minimize steering angle drift. Future research focuses on the investigation of the differences between controllers' performances during more complex maneuvers with speed and road friction variation.

APPENDIX A
NEUROMUSCULAR SYSTEM PARAMETERS

The values of the NMS system parameters and their source are reported in Table V.

APPENDIX B
KRUSKAL-WALLIS TEST - DIL

The Kruskal-Wallis test is a rank-based non-parametric test commonly used to determine if there are statistically significant differences between two or more groups of an independent variable on a dependent variable [43].

TABLE VII
KRUSKAL-WALLIS TEST - ANGLE HYSTERESIS SINE SECTIONS

Section	**PBC**	**TBC**	**TBC + noise**	**H**	**p**
1	3.69 (0.25)	3.38 (0.23)	3.07 (0.25)	**13.28**	**0.001**
2	3.63 (0.17)	3.44 (0.11)	3.25 (0.12)	**13.31**	**0.001**
3	4.8 (0.51)	4.22 (0.54)	(3.74) (0.55)	**10.2**	**0.007**
4	4.24 (0.25)	3.66 (0.41)	3.47 (0.24)	**10.2**	**0.006**

TABLE VIII
KRUSKAL-WALLIS TEST - TORQUE HYSTERESIS SINE SECTIONS

Section	**PBC**	**TBC**	**TBC + noise**	**H**	**p**
1	1.13 (0.09)	0.91 (0.1)	0.86 (0.07)	**13.55**	**0.001**
2	1.51 (0.08)	1.29 (0.07)	1.27 (0.06)	**12.31**	**0.002**
3	1.12 (0.13)	0.94 (0.14)	0.86 (0.05)	**11.62**	**0.003**
4	1.27 (0.08)	1.07 (0.09)	1.01 (0.06)	**12.76**	**0.002**

TABLE IX
KRUSKAL-WALLIS TEST - SUBJECTIVE DATA

Criteria	**PBC**	**TBC**	**TBC + noise**	**H**	**p**
Overall effort	5.6 (0.52)	3.7 (0.76)	3.6 (1.19)	**13.51**	**0.001**
Steering solidity	5.6 (0.79)	4.1 (1.73)	3.9 (1.25)	**6.45**	**0.040**
Holding precision	3.6 (1.38)	5.1 (0.69)	5.4 (0.53)	**8.06**	**0.017**
Vibrations	5.8 (0.92)	3.3 (0.76)	4.3 (0.70)	**15.11**	**0.001**
Steering realism	2.7 (0.70)	3.8 (1.51)	5.0 (0.76)	**12.12**	**0.002**

Tables VI - IX report the H and p values of the Kruskal-Wallis test for the objective and subjective indicators of the DiL experiment.

APPENDIX C
BOX PLOT DIL EXPERIMENT

See Fig. 15.

ACKNOWLEDGMENT

The authors are grateful to Toyota Motor Europe and the Delft University of Technology for enabling the publication of this work and the active involvement which lead to its realization.

REFERENCES

[1] J. de Winter, P. van Leeuwen and R. Happee, "Advantages and disadvantages of driving simulators: A discussion," in *Proc. Measuring Driving Behav.*, The Netherlands, 2012, pp. 47–50.

[2] I. A. Badiru, "Customer focus in EPS steering feel development," *Int. J. Passenger Cars- Mech. Syst.*, SAE, vol. 7, no. 3, pp. 1009–1015, 2014.

[3] S. T. Godley, T. J. Triggs, and B. N. Fildes, "Driving simulator validation for speed research," *Accident Anal. Prevention*, Elsevier, vol. 34, no. 5, pp. 589–600, 2002.

[4] T. J. Triggs, "Some critical human factors issues and challenges in simulation and training," in *Proc. Simtect Conf.*, CRC Press, 1996, pp. 21–26.

[5] G. J. Blaauw, "Driving experience and task demands in simulator and instrumented car: A validation study," *Hum. Factors*, *SAGE*, vol. 24, no. 4, pp. 473–486, 1982.

[6] A. Kemeny and F. Panerai, "Evaluating perception in driving simulation experiments," *Trends Cogn. Sci.*, Elsevier, vol. 7, no. 1, pp. 31–37, 2003.

[7] Y. Khusro, Y. Zheng, M. Grottoli, and B. Shyrokau, "MPC-based motion-cueing algorithm for a 6-DOF driving simulator with actuator constraints," *Vehicles*, MDPI, vol. 2, no. 4, pp. 625–647, 2020.

[8] B. H. Philips and T. Morton, "Making driving simulators more useful for behavioral research: Simulator characteristics comparison and model-based transformation," Summary Report No. FHWA-HRT-15-016, U.S. Dept. Transp., Federal Highway Admin., Office of Safety Research and Development, 2015.

[9] P. Bouchner and S. Novotny, "Development of advanced driving simulator: Steering wheel and brake pedal feedback," in *Proc. 2nd Int. Conf. Circuits, Syst., Control, Signals*, 2011, pp. 170–174.

[10] D. Toffin, G. Reymond, A. Kemeny, and J. Droulez, "Role of steering wheel feedback on driver performance: Driving simulator and modeling analysis," *Veh. Syst. Dyn.*, Taylor & Francis, vol. 45, no. 5, pp. 375–388, 2007.

[11] P. E. Pfeffer, M. Harrer, and D. N. Johnston, "Interaction of vehicle and steering system regarding on-centre handling," *Veh. Syst. Dyn.*, Taylor & Francis, vol. 46, no. 5, pp. 413–428, 2008.

[12] L. Chen and A. G. Ulsoy, "Experimental validation of a robust steering assist controller on a driving simulator," in *Proc. Amer. Control Conf.*, 2002, pp. 2528–2533.

[13] R. Mourant and P. Sandhu, "Evaluation of force feedback steering in a fixed based driving simulator," in *Proc. Hum. Factors Ergonom. Soc. Annu. Meeting*, SAGE, 2002, vol. 46, pp. 2202–2205.

[14] B. Shyrokau, J. Loof, O. Stroosma, M. Wang, and R. Happee, "Effect of steering model fidelity on subjective evaluation of truck steering feel," in *Proc. Driving Simulator Conf. Europe*, Tübingen, Germany, 2015, pp. 16–18.

[15] T. Chugh, F. Bruzelius, M. Klomp, and B. Shyrokau, "An approach to develop haptic feedback control reference for steering systems using open-loop driving manoeuvres," *Veh. Syst. Dyn.*, Taylor & Francis, vol. 58, no. 12, pp. 1953–1976, 2020.

[16] M. Damian, B. Shyrokau, A. Ocariz, and X. A. Carrera, "Torque control for more realistic hand-wheel haptics in a driving simulator," in *Proc. Driving Simul. Conf.*, Strasbourg, France, 2019, pp. 4–6.

[17] G. Gritti *et al.*, "Mechanical steering gear internal friction: Effects on the drive feel and development of an analytic experimental model for its prediction," in *Advances on Mechanics, Design Engineering and Manufacturing*. Cham, Switzerland: Springer, 2007, pp. 339–350.

[18] C. Certosini, F. Vinattieri, R. Capitani, and C. Annicchiarico, "Development of a real-time steering system model for driving simulators," *Proc. Institution Mech. Engineers, Part D, J. Automobile Eng.*, London, U.K., SAGE, vol. 233, no. 11, pp. 2701–2713, 2019.

[19] D. A. Haessig and B. Friedland, "On the modeling and simulation of friction," *Proc. SPIE*, San Diego, CA, USA, vol. 1482, no. 3, pp. 383–396, 1990.

[20] D. A. Abbink, S. Kolekar, and J. D. Winter, "A human-like steering model: Sensitive to uncertainty in the environment," in *Proc. Int. Conf. Syst., Man, Cybern.*, Banff, Canada, 2017, pp. 1487–1492.

[21] D. A. Abbink and M. Mulder, "Neuromuscular analysis as a guideline in designing shared control," in *Advances in Haptics*. London, U.K.: IntechOpen, 2010.

[22] D. Katzourakis, C. Droogendijk, D. A. Abbink, R. Happee, and E. Holweg, "Force-feedback driver model for objective assessment of automotive steering systems," in *Proc. 10th Int. Symp. Adv. Veh. Control*, 2010, pp. 381–386.

[23] W. Hoult and D. J. Cole, "A neuromuscular model featuring co-activation for driver simulation," *Int. J. Veh. Mech. Mobility*, Taylor & Francis, vol 46, pp. 175–189, 2008.

[24] D. J. Cole, "A path-following driver-vehicle model with neuromuscular dynamics, including measured and simulated responses to a step in steering angle overlay," *Veh. Syst. Dyn.*, Taylor & Francis, vol. 50, no. 4, pp. 573–596, 2012.

[25] A. M. R. Lazcano, T. Niu, X. A. Carrera, and B. Shyrokau, "MPC-based haptic shared steering system: A driver modelling approach for symbiotic driving," *ASME Trans. Mechatronics*, vol. 26, no. 3, pp. 1201–1211, 2021.

[26] D. W. Franklin, R.. Osu, E. Burdet, M. Kawato, and E. T. Milner, "Adaptation to stable and unstable dynamics achieved by combined impedance control and inverse dynamics model,"*J. Neuriophysiol.*, American Physiological Society, vol. 90, no. 5, pp. 3270–3282, 2003.

[27] D. Katzourakis, "Driver steering support interfaces near the vehicleś handling limits," Ph.D. dissertation, Delft Univ. Technol., The Netherlands, 2012.

[28] W. Mugge, D. Abbink, A. C. Schouten, J. P. DeWald, and F. C. T. vd Helm, "A rigorous model of reflex function indicates that position and force feedback are flexibly tuned to position and force tasks," *Exp. Brain Res.*, vol. 200, no. 3, pp. 325–340, 2010.

[29] R. Happee, A. C. Schouten, and E. de Vlugt, "Posture maintenance of the human upper extremity; Identification of intrinsic and reflex based contributions," *SAE Int. J. Passenger Cars*, vol. 1, pp. 1125–1135, 2008.

[30] J. M. Winters and L. Stark, "Estimated mechanical-properties of synergistic muscles involved in movements of a variety of human joints,"*J. Biomech.*, vol. 21, no. 12, pp. 1027–1041, 1988.

[31] A. C. Schouten, W. Mugge, and F. C. T. vd Helm, "NMClab a model to assess the contributions of muscle visco-elasticity and afferent feedback to joint dynamics," *J. Biomech.*, vol. 41, pp. 1659–1667, 2008.

[32] G. Mastinu, M. Gobbi, F. Comolli, and M. Hada, "Instrumented steering wheel for accurate ADAS development," SAE Tech. Paper, Rep. no. 2019-01-1241, 2019.

[33] X. A. Carrera, O. Kimiaki, F. Comolli, M. Gobbi, and G. Mastinu, "Further understanding of steering feedback and driver behavior through the application of an instrumented steering wheel," *Proc. Int. Munich Chassis Symp.*, no. 10, pp. 481–502, 2019.

[34] Y. Jiang, W. Deng, J. Wu, S. Zhang, and R. He, "Study on the stability of the steering torque feedback system considering the time delay and the system characteristics," *Proc. Inst. Mech. Engineers Part D, J. Automobile Eng.*, SAGE, vol. 232, no. 5, pp. 707–721, 2018.

[35] B. Shyrokau *et al.*, "The effect of steering-system linearity and simulator motion on truck steering," *Appl. Ergonom.*, Elsevier, vol. 71, pp. 17–28, 2018.

[36] F. E. Jaksch, "Driver-vehicle interaction with respect to steering controllability," SAE Tech. Paper, SAE, Rep. no. 790740, pp. 2592–2629, 1979.

[37] P. Green, B. Cullinane, B. Zylstra, and D. Smith, "Typical values for driving performance with emphasis on the standard deviation of lane position: A summary of the literature," Univ. Michigan Transp. Res. Inst., 2003. [Online]. Available: https://www.volpe.dot.gov/safety-management-and-human-factors/surface-transportation-human-factors/typical-values-driving

[38] O. Nakayama, T. Futami, T. Nakamura and E. R. Boer, "Development of a steering entropy method for evaluating driver workload," *SAE Trans.*, SAE, vol. 108, pp. 1686–1695, 1999.

[39] P. Green, "Standard definitions for driving measures and statistics: overview and status of recommended practice J2944," in *Proc. 5th Int. Conf. Automot. User Interfaces Interactive Veh. Appl.*, 2013, pp. 184–191.

[40] International Standard Organization, "Road vehicle . Test method for the quantification of on-centre handling . Part 1: Weave test," ISO 13674-1, 2003.

[41] M. Koide and S. Kawakami, "Analysis of "steering feel" evaluation in vehicles with power steering," *JSAE Rev.*, vol. 9, no. 3, pp. 36–42, 1988.

[42] J. Taylor, *Introduction to Error Analysis, The Study of Uncertainties in Physical Measurements*. Herndon, VA, USA: Univ. Sci. Books, pp. 141–146, 1997.

[43] E. Ostertagová, O. Ostertag, and J. Kováč,"Methodology and application of the Kruskal-Wallis test," *Appl. Mech. Mater.*, vol. 611, pp. 115–120, 2014.

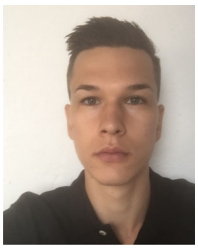

Mircea Damian received the bachelor's degree in engineering sciences, with a specialization in mechanical engineering from the University of Rome Tor Vergata, Rome, Italy, in 2017 and the M.Sc. degree (*cum laude*) in mechanical engineering, with specialisation in vehicle engineering from the Delft University of Technology, Delft, The Netherlands, in 2019. Since 2020, he has been a Junior Manager Trainee with Bosch Romania.

His research interests include steering dynamics, driver modeling, control feedback, and driving simulator technologies.

Barys Shyrokau received the Dipl.Eng. degree (*cum laude*) in mechanical engineering from Belarusian National Technical University, Minsk, Belarus, in 2004 and the joint Ph.D. degree in control engineering from the Nanyang Technological University, Singapore, and Technical University of Munich, Munich, Germany, in 2015. He is currently an Assistant Professor with the Section of Intelligent Vehicles, Department of Cognitive Robotics, Delft University of Technology, Delft, The Netherlands, and involved in research related to vehicle dynamics and control, motion comfort, and driving simulator technology. He is scholarship and award holder of FISITA, DAAD, SINGA, ISTVS, and CADLM.

Xabier Carrera Akutaín received the Ph.D. degree in mechanical engineering from the University of Navarra, Pamplona, Spain, in 2006. In 2009, he started working with Toyota Motor Europe, Belgium, as a Senior Engineer of vehicle dynamics. From 2013 to 2015, he was an Expert Vehicle Dynamics with Toyota Motor Corporation, Japan. Since 2016, he has been the Manager of Vehicle Dynamics and Virtual Evaluation Group, TME, Belgium. His research interests include human perception of performance metrics and driving simulator toolchain development.

Riender Happee received the M.Sc. degree in mechanical engineering and the Ph.D. degree from the Delft University of Technology, Delft, The Netherlands, in 1986 and 1992, respectively. During 1992–2007, he investigated road safety and introduced biomechanical human models for impact and comfort with TNO Automotive. He is currently investigates the human interaction with automated vehicles focusing on safety, comfort and acceptance with the Delft University of Technology, where he is an Associate Professor with the Faculties of Mechanical, Maritime and Materials Engineering, and Civil Engineering and Geosciences.